



Integrated framework for characterization of spatial variability of geological profiles

Journal:	<i>Canadian Geotechnical Journal</i>
Manuscript ID	cgj-2016-0189.R2
Manuscript Type:	Article
Date Submitted by the Author:	01-Aug-2016
Complete List of Authors:	Liu, Wenfei; The Hong Kong Polytechnic University, Civil and Environmental Eng Leung, Yat Fai; The Hong Kong Polytechnic University, Civil and Environmental Eng Lo, Man Kong; The Hong Kong Polytechnic University, Civil and Environmental Eng
Keyword:	site investigation, Restricted Maximum Likelihood method, Matérn covariance structure, Residual analysis, Rockhead variation
<p>Note: The following files were submitted by the author for peer review, but cannot be converted to PDF. You must view these files (e.g. movies) online.</p> <p>CanGeotech_production.tex nrc.dtx nrc.ins</p>	

SCHOLARONE™
Manuscripts

Integrated framework for characterization of spatial variability of geological profiles

W.F. Liu¹, Y.F. Leung^{1*}, and M.K. Lo¹

¹Department of Civil and Environmental Engineering, The Hong Kong Polytechnic University, Hong Kong

*Corresponding author, email address: yfleung@polyu.edu.hk

ABSTRACT

Despite recent efforts to characterize the uncertainties involved with geological profiles and soil and rock properties, there has been limited study on their spatial correlations and how such features may be included in the engineering decision-making process. This paper presents an integrated framework for geostatistical analyses, which incorporates the Restricted Maximum Likelihood (REML) method with the Matérn autocovariance model. Statistical tests are conducted including those for data normality, constant variance and outliers, which ensure the fundamental assumptions of REML are not violated in the residual analyses of site data, meanwhile offering simple checks for potential errors in the dataset. The proposed approach also allows quantification of uncertainties in the subsurface profiles at the unsampled locations. The approach is illustrated through investigations on spatial correlation features of geological profiles at two project sites in Hong Kong. The numbers of irregularly-spaced boreholes vary from 150 to 350 in the two cases, and the large volume of data enables the variations in rockhead levels to be studied through the proposed framework. In addition, the existence of geological faults in one of the sites is found to significantly affect the spatial variability of rockhead level, as indicated by the reduced scales of fluctuation and spatial dependence, which corresponds to increased uncertainty in areas intersected by faults.

Keywords: Site investigation, Restricted Maximum Likelihood method, Matérn covariance structure, Residual analysis, Rockhead variation

1 INTRODUCTION

2 Uncertainties in soil profiles and their properties are often the cause of geotechnical
3 problems encountered during construction. For example, Clayton (2001) conducted a survey
4 of 28 construction projects in the United Kingdom, which revealed that many geotechnical
5 problems encountered during construction stemmed from uncertainties regarding boundaries
6 of the soil strata (22%) and properties of the geo-materials (20%). However, studies on the
7 spatial variability or correlation of soil properties have been hampered by the lack of data.
8 Christian and Baecher (2011) stated that the “unresolved problems in geotechnical risk and
9 reliability” included uncertainties in the variability and spatial correlations of geotechnical
10 properties.

11 DeGroot (1996) compiled the results from a number of earlier studies, and reported
12 the correlation distances of geotechnical properties including undrained shear strengths
13 and CPT cone tip resistance. Phoon and Kulhawy (1999a,b) also reported the scales of
14 fluctuation of various soil properties, without describing the details of spatial correlation
15 structure. The correlation structure of geotechnical data is sometimes analyzed through the
16 autocorrelation (Vanmarcke 1977; DeGroot and Baecher 1993) or by geostatistics (Matheron
17 1971), as illustrated in the works by Soulié et al. (1990), Chiasson et al. (1995) and Wang
18 and Chiasson (2006), etc. In these analyses, it is common for researchers to assume certain
19 functional form for the autocorrelation structure (e.g., Gaussian or spherical), and then
20 estimate the parameters for the assumed function (Elkateb et al. 2003; Phoon et al. 2004;
21 Stuedlein et al. 2012; Firouziandbandpey et al. 2014). However, the validity of such assumption
22 have not been discussed in detail. Alternatively, Bayes' Theorem can be applied to determine
23 the most probable correlation function of the spatial data through weighting their posterior
24 probabilities, as illustrated by Cao and Wang (2013, 2014) and Wang et al. (2010, 2013, 2014,
25 2015, 2016), who adopted the approach in characterizing underground soil stratification and
26 variability of geotechnical properties.

27 Contrary to the Bayesian approach, this paper presents an integrated framework which

28 ensures the available geotechnical data is best utilized in rigorous statistical analyses. For
29 example, Phoon et al. (2003) stated that stationarity is an important prerequisite for
30 geostatistical analyses, and proposed the use of Modified Bartlett test statistic as a basis
31 to reject the null hypothesis of stationarity. However, many previous studies did not verify
32 stationarity in the data. Also, a constant mean for the residuals is a necessary condition for
33 stationarity, and certain fixed polynomial order is usually assumed in the detrending process
34 (Stuedlein et al. 2012). For example, Liu and Leung (2015) presented the preliminary analyses
35 of the spatial data of geological profiles assuming quadratic and cubic trend structures, but
36 stationarity assumption was not confirmed in the analyses.

37 The current study proposes a new integrated framework and procedures that incorporate
38 data transform and rigorous residual analyses to ensure stationarity assumptions are satisfied,
39 thereby enhancing the reliability of residual analysis. The framework also enables rational
40 detrending process with the optimal polynomial order, and detection of outliers in the
41 dataset which are not considered in previous attempts to characterize ground variability. The
42 Matérn function (Matérn 1960) is adopted to model the autocorrelation structures, owing
43 to the flexibility of its functional form. Parameters of the function are optimized using a
44 heuristic algorithm, known as the Differential Evolution (Storn and Price 1997), to maximize
45 the log-likelihood value under the Restricted Maximum Likelihood (REML) method. The
46 proposed framework can be used to evaluate the spatial variations of soil and rock strata,
47 obtaining parameters such as the spatial dependence and scale of fluctuation using site-specific
48 information. To illustrate the capabilities of the approach, information on the engineering
49 rockhead level (moderately weathered granite) from irregularly-spaced boreholes at two sites
50 in Hong Kong is analyzed to reveal their spatial variability characteristics. This study also
51 discusses the impacts of the existence of geologic features, such as faults, on the variability of
52 geological profiles.

53 **PROPOSED FRAMEWORK FOR RESIDUAL ANALYSIS**

54 Spatial random variables are often expressed as a combination of fixed effects and random

55 effects, also known as the deterministic trend structure and the residual effects. With \mathbf{x}
 56 representing the spatial coordinates of sampled points, a general linear mixed regression
 57 model for spatial data, $\mathbf{z}(\mathbf{x})$, can be formulated by:

$$\mathbf{z}(\mathbf{x}) = \mathbf{X}\boldsymbol{\beta} + \boldsymbol{\varepsilon} \quad (1)$$

58 where $\mathbf{X}\boldsymbol{\beta}$ represents the large scale trend, with \mathbf{X} being the deterministic component matrix
 59 that contains information on spatial coordinates. $\boldsymbol{\beta}$ is the vector of regression coefficients
 60 according to the corresponding trend structure (linear, quadratic, cubic, etc.). The residual,
 61 $\boldsymbol{\varepsilon}$, is a combination of the correlation structure (with smooth scale variation of variance σ_e^2)
 62 and a white noise process (with variance σ_n^2), since white noise effects are assumed not to
 63 correlate with distance. The covariance matrix of $\boldsymbol{\varepsilon}$ is related to the correlation structure, \mathbf{R} ,
 64 by:

$$\mathbf{V} = \mathbf{Var}(\boldsymbol{\varepsilon}) = \sigma_e^2 \mathbf{R} + \sigma_n^2 \mathbf{I} = (\sigma_e^2 + \sigma_n^2) [s\mathbf{R} + (1-s)\mathbf{I}]$$

$$\text{where } 0 \leq s = \frac{\sigma_e^2}{\sigma_e^2 + \sigma_n^2} \leq 1 \quad (2)$$

65 In Eq. (2), \mathbf{I} is the identity matrix, and s is the spatial dependence which incorporates
 66 the nugget effect (due to white noise) into the covariance model. Previously, the correlation
 67 structure, i.e., individual components of \mathbf{R} , is often assumed to follow a certain fixed function,
 68 such as the Gaussian, exponential or spherical function (DeGroot and Baecher 1993). In the
 69 current study, in order to allow flexibility in the functional form of \mathbf{R} , the Matérn function is
 70 adopted as follows (Matérn 1960):

$$R(h_{ij}) = \frac{1}{2^{\nu-1}\Gamma(\nu)} \left(\frac{h_{ij}}{r}\right)^{\nu} K_{\nu}\left(\frac{h_{ij}}{r}\right) \quad (3)$$

71 where h_{ij} is the separation distance between points i and j , ν is a smoothness parameter
 72 ranging from 0 to infinity, r is the range parameter, Γ is the gamma function, and K_{ν}

73 represents the modified Bessel function of the second kind with order ν .

74 The Matérn function is a generalized function with its shape controlled by the smoothness
75 parameter. For example, it corresponds to the exponential function when $\nu = 0.5$, and is
76 equivalent to the Gaussian function when ν approaches infinity (Minasny and McBratney
77 2005). The scale of fluctuation, δ , of the Matérn function is determined by both ν and r . In
78 this paper, it is taken as the separation distance where the autocorrelation, $sR(h_{ij})$, equals
79 $0.05s$ (Elkateb et al. 2003; Rue and Held 2005), and Fig. 1 shows the relationship between ν ,
80 r and δ accordingly. Also, it should be noted that some researchers proposed a different form
81 for the Matérn function (Stein 1999), but the resulting estimates of scales of fluctuation are
82 essentially the same.

83 The framework proposed in this study consists of three key components, namely REML
84 analysis with Box-Cox transformation, trend structure determination and statistical tests
85 for residuals. These components, particularly the latter two, have not been considered in
86 previous studies such as Haskard (2007) or existing software such as ArcGIS and geoR. Fig. 2
87 shows a flowchart of the framework, and the three components are discussed in the following
88 sections.

89 **Restricted Maximum Likelihood (REML)**

90 To ensure stationarity of the spatial data, it is important to estimate and remove the
91 trend (or fixed effects, $\mathbf{X}\beta$), so that the spatial correlation features are not masked by this
92 deterministic component. In some previous studies, the trend component is determined
93 by regression analysis using linear or polynomial functions (Dasaka and Zhang 2012; Lark
94 et al. 2006), and the residuals are then analysed and presented using method of moments
95 or semivariograms. However, the semivariance estimates are not unique when the samples
96 are irregularly spaced, as the semivariance can be affected by subjective decisions on the
97 lag size (bin size). Also, the subsequent semivariograms are estimated through a subjective
98 curve-fitting process.

99 In the current study, the Restricted Maximum Likelihood (REML) method is applied to

100 simultaneously determine the trend coefficients and estimate the autocorrelation properties
 101 of residuals. The method does not require decisions on the bin size so it can be applied to
 102 irregularly-spaced sampling points. An important assumption in the development of REML
 103 methods is that the data follows a normal distribution, and that the variance of residuals
 104 is constant throughout the domain. These assumptions are often made, but rarely verified,
 105 in most previous studies. In the current work, the Box-Cox transformation (Box and Cox
 106 1964) is performed on the raw dataset, \mathbf{z}^* , to ensure these assumptions are satisfied. The
 107 transformed dataset, \mathbf{z} , can be represented by the following equation:

$$z_i = \begin{cases} \frac{(z_i^* + \lambda_2)^{\lambda_1} - 1}{\lambda_1 (gm(\mathbf{z}^* + \boldsymbol{\lambda}))^{(\lambda_1 - 1)}} & \text{if } \lambda_1 \neq 0 \\ (gm(\mathbf{z}^* + \boldsymbol{\lambda})) \log(z_i^* + \lambda_2) & \text{if } \lambda_1 = 0 \end{cases} \quad (4)$$

108 where $\boldsymbol{\lambda}$ is a vector with all the terms equal to λ_2 , which is a parameter used to ensure
 109 $z_i^* + \lambda_2 > 0$. λ_1 is estimated by minimizing the residual sum of squares (RSS) of \mathbf{z} , and $gm(\cdot)$
 110 denotes the geometric mean of the vector $\mathbf{z}^* + \boldsymbol{\lambda}$.

111 Details of the REML approach have been described in Cressie and Lahiri (1996) and Lark
 112 and Cullis (2004). In short, the autocorrelation structure can be obtained by maximizing the
 113 following log-likelihood function with respect to $\boldsymbol{\theta}$:

$$L(\boldsymbol{\theta}|\mathbf{y}) = -\frac{n-p}{2} \log(2\pi) - \frac{1}{2} \log|\mathbf{V}| - \frac{1}{2} \log|\mathbf{W}| - \frac{1}{2} \mathbf{y}^T \mathbf{V}^{-1} \mathbf{Q} \mathbf{y} \quad (5)$$

114 where $\mathbf{W} = \mathbf{X}^T \mathbf{V}^{-1} \mathbf{X}$ and $\mathbf{Q} = \mathbf{I} - \mathbf{X} \mathbf{W}^{-1} \mathbf{X}^T \mathbf{V}^{-1}$. $\boldsymbol{\theta}$ represents the unknown quantities in the
 115 autocorrelation structure, i.e., s , ν and r in Eqs. (2) and (3). In Eq. (5), n is the number of data
 116 points, and p is the number of coefficients in the trend structure. $\mathbf{y} = (\mathbf{I} - \mathbf{X}(\mathbf{X}^T \mathbf{X})^{-1} \mathbf{X}^T) \mathbf{z}$,
 117 which is the matrix of filtered dataset with the trend components filtered out. Therefore, the
 118 covariance estimates of REML are independent of the trend estimates.

119 The determination of $\boldsymbol{\theta}$ can be treated as an optimization problem, aiming to obtain the
 120 set of $\{s, \nu, r\}$ parameters that maximize the log-likelihood function. In the current work,

121 this is achieved using the Differential Evolution algorithm (Storn and Price 1997). This is
 122 conceptually similar to other evolutionary algorithms, which is not prone to converging at
 123 local maxima, and has recently been applied in a number of engineering problems.

124 Once the covariance structure is determined, the trend coefficients, and subsequently the
 125 predicted residuals, can be estimated using generalized least squares (GLS):

$$\hat{\boldsymbol{\beta}} = (\mathbf{X}\mathbf{V}^{-1}\mathbf{X}^T)^{-1}\mathbf{X}\mathbf{V}^{-1}\mathbf{z} \quad (6)$$

126

$$\hat{\boldsymbol{\varepsilon}} = \mathbf{z} - \mathbf{X}\hat{\boldsymbol{\beta}} \quad (7)$$

127 The predictions at unsampled locations, $\hat{z}(\mathbf{x}_0)$, and the corresponding prediction variance,
 128 $\sigma_z^2(\mathbf{x}_0)$, can be estimated based on the Best Linear Unbiased Prediction (BLUP) technique
 129 (Atkinson et al. 2008; Santra et al. 2012):

$$\hat{z}(\mathbf{x}_0) = \mathbf{X}_0^T \hat{\boldsymbol{\beta}} + \mathbf{K}^T \mathbf{V}^{-1} \hat{\boldsymbol{\varepsilon}} \quad (8)$$

130

$$\sigma_z^2(\mathbf{x}_0) = \text{diag}(\mathbf{K}_0 - \mathbf{K}^T \mathbf{V}^{-1} \mathbf{K} + \mathbf{M}^T (\mathbf{X}\mathbf{V}^{-1} \mathbf{X}^T)^{-1} \mathbf{M}) \quad (9)$$

131 where \mathbf{X}_0 is the deterministic component matrix of prediction. \mathbf{K} represents the covari-
 132 ance matrix between observations and predictions, i.e., $\mathbf{K} = \text{cov}\{z(\mathbf{x}), z(\mathbf{x}_0)\}$, $\mathbf{K}_0 =$
 133 $\text{cov}\{z(\mathbf{x}_0), z(\mathbf{x}_0)^T\}$ and $\mathbf{M} = \mathbf{X}_0 - \mathbf{X}\mathbf{V}^{-1}\mathbf{K}$.

134 It should be noted that the predictions and associated variance evaluated by Eqs. (8) and
 135 (9) correspond to values in the ‘transformed’ space, under Box-Cox transformation. While
 136 $\hat{z}(\mathbf{x}_0)$ can be back-transformed to the original space through Eq. (4), back-transformation of
 137 the prediction variance can be approximated by multiplying $\sigma_z^2(\mathbf{x}_0)$ with a factor Φ (Cressie
 138 1993). For unsampled location i :

$$\Phi_i = (\lambda_1 gm(z)^{\lambda_1 - 1} (\lambda_1 gm(z)^{\lambda_1 - 1} (\mathbf{X}_0 \hat{\boldsymbol{\beta}})_i + 1)^{\frac{1}{\lambda_1} - 1})^2 \quad (10)$$

139 As will be shown in the following case study, the distributions of prediction variances in
140 the transformed and back-transformed (original) spaces are broadly similar.

141 **Regression diagnostics for REML**

142 *Normality*

143 The Box-Cox transformation (Eq. (4)) minimizes the recovered residuals but does not
144 guarantee normality – the approach assumes that the transformed data has the highest
145 likelihood to be normally distributed when RSS value of \mathbf{z} is minimized. It is therefore
146 necessary to perform diagnostics for normality to ensure the assumption of REML is not
147 violated.

148 Traditional diagnostics for normal errors in regression typically utilize ordinary residuals,
149 based on uncorrelated linear mixed model. The residuals after GLS process, however,
150 are correlated spatially, according to the autocovariance model effects. Therefore, the
151 GLS residuals need to be converted to recovered residuals before executing the normality
152 diagnostics. The current study applied the Kolmogorov-Smirnov (KS) test to diagnose the
153 normality of residuals (Smirnov 1939; Jensen and Ramirez 1999). The KS test evaluates
154 the maximum deviation between the cumulative distribution of the recovered residuals and
155 that of a theoretical normal distribution. The P_N value is defined as the tail probability for
156 this deviation to be small enough for the data to be considered normally distributed. In the
157 current study, a P_N value exceeding 0.05 is considered to satisfy the normality assumption.

158 *Constant variance*

159 After removing the deterministic trend component ($\mathbf{X}\boldsymbol{\beta}$), the residuals ($\boldsymbol{\varepsilon}$) are assumed to
160 be stationary in the REML formulation, which implies a constant variance across the domain.
161 However, the validity of this assumption has rarely been verified in previous applications of
162 geostatistical methods.

163 The Breusch-Pagan Test (Breusch and Pagan 1979) is frequently used in statistics to
164 verify the constant variance assumption. During the test, a regression is conducted on the
165 squared residuals with the explanatory variables (i.e. across the spatial coordinates in this

166 case), and it checks whether a trend exists in the variance. The null hypothesis, H_0 , is defined
 167 by all regression coefficients of the variances being zero. The P_C value is defined as the tail
 168 probability for the regression coefficients to be considered insignificant. In the current study,
 169 a P_C value exceeding 0.05 corresponds to acceptance of H_0 , and the data is considered to
 170 satisfy the constant variance assumption.

171 The original Breusch-Pagan test is based on residuals obtained from ordinary least squares
 172 (OLS), where spatial correlation is absent. To apply this test to the general linear mixed
 173 model, the spatial correlation effect has to be removed from the residuals. This is achieved in
 174 the current study by multiplying the negative square root of the covariance matrix to the
 175 GLS residuals:

$$\boldsymbol{\varepsilon}^* = \mathbf{V}^{-\frac{1}{2}} \hat{\boldsymbol{\varepsilon}} = \mathbf{P} \mathbf{O}^{-\frac{1}{2}} \mathbf{P}^T \hat{\boldsymbol{\varepsilon}} \quad (11)$$

176 where $\boldsymbol{\varepsilon}^*$ is Pearson residuals for constant variance test, $\hat{\boldsymbol{\varepsilon}}$ is predicted residuals calculated by
 177 Eq. (7), \mathbf{P} is the square matrix containing the eigenvectors of covariance matrix \mathbf{V} , and \mathbf{O} is
 178 the diagonal matrix containing the eigenvalues of \mathbf{V} . The Breusch-Pagan test is then applied
 179 to $\boldsymbol{\varepsilon}^*$ of the uncorrelated model.

180 *Detection of potential outliers*

181 Outliers are data points that vary significantly from the neighboring points in the spatial
 182 context, and can be indications of peculiarities or errors in the dataset which influence
 183 geostatistical analyses. For example, Lark (2000) stated that the maximum likelihood
 184 method was susceptible to asymmetry caused by outliers. There are multiple methods for
 185 detection of outliers, and this is achieved by two approaches in the current study. The first
 186 approach examines the distribution of residuals ($\hat{\boldsymbol{\varepsilon}}$) in the spatial domain, and the data points
 187 with residuals exceeding ± 1.96 times their standard deviation ($\sqrt{\sigma_e^2 + \sigma_n^2}$) are identified as
 188 potential outliers. This represents the 95% inter-percentile range assuming the residuals
 189 follow a normal distribution, and those outside this range may be considered ‘extreme’ values
 190 of deviations from the trend.

191 The second approach evaluates the Cook's distance (Cook 1977) of each data point, which
 192 is an indicator of its influence to regression results. The Cook's distance is based on the
 193 difference between regression coefficients estimated with all the observations, i.e., $\hat{\beta}$; and
 194 coefficients estimated without a particular observation i , i.e., $\hat{\beta}(i)$ (Haslett and Hayes 1998).
 195 This difference is often termed **DFBETA**, and is referred to as **D** herein for simplicity.
 196 A large value of D_{ji} suggests that the i^{th} data point is influential in determining the j^{th}
 197 regression coefficient, which may indicate an outlying data point. D_{ji} can be estimated by:

$$D_{ji} = \frac{\hat{\beta}_j - \hat{\beta}_j(i)}{\sqrt{\text{Var}(\hat{\beta})_{jj}}} = \frac{\mathbf{B}_{ji} \tilde{\epsilon}_i}{\sqrt{\text{Var}(\hat{\beta})_{jj}}}$$

where $\mathbf{B} = \mathbf{W}^{-1} \mathbf{X}^T \mathbf{V}^{-1}$

$$\tilde{\epsilon} = [\mathbf{I} \text{diag}(\mathbf{E})]^{-1} \mathbf{E} \mathbf{z}$$

$$\mathbf{E} = \mathbf{V}^{-1} - \mathbf{V}^{-1} \mathbf{X} \mathbf{W}^{-1} \mathbf{X}^T \mathbf{V}^{-1} \quad (12)$$

198 where $\text{diag}(\mathbf{E})$ is a vector consisting of the diagonal components of \mathbf{E} . D_{ji} measures the
 199 change of the j^{th} individual regression coefficient when the i^{th} observation is deleted, scaled
 200 by the variance of $\hat{\beta}$, which is $\text{Var}(\hat{\beta}) = \mathbf{W}^{-1}$, and the subscript jj indicates the j^{th} diagonal
 201 element of $\text{Var}(\hat{\beta})$. Therefore, the D_i vector summarizes the changes in all regression
 202 coefficients resulting from deleting the i^{th} observation.

203 The Cook's distance is defined as the average of the squared D_{ji} components, which is
 204 proportional to the squared length of the D_i vector. For example, the Cook's distance for
 205 the i^{th} observation point can be expressed as:

$$C_i = \frac{1}{p} \sum_{j=1}^p D_{ji}^2 = \frac{1}{p} \sum_{j=1}^p \left[\frac{\hat{\beta}_j - \hat{\beta}_j(i)}{\sqrt{\text{Var}(\hat{\beta})_{jj}}} \right]^2 = \frac{(\hat{\beta} - \hat{\beta}(i))^T (\hat{\beta} - \hat{\beta}(i))}{p \text{Var}(\hat{\beta})_{jj}} \quad (13)$$

206 where p is the number of regression coefficients. Belsley et al. (2005) suggested $2/\sqrt{n}$ as the
 207 cutoff value for D_{ji} for outlier diagnostics. Correspondingly, the cutoff value for C_i can be
 208 taken as $(2/\sqrt{n})^2 = 4/n$ (Nieuwenhuis et al. 2012). In other words, an observation point i is

209 classified as an outlier if $C_i > 4/n$.

210 The necessity and implementation of the two approaches for outlier detection will be
211 illustrated through the NTK case study described in later sections.

212 **Determination of polynomial order of trend structure**

213 The REML approach, together with GLS, allow determination of the trend coefficients $\hat{\beta}$.
214 However, the polynomial order of the trend structure (i.e. the size of $\hat{\beta}$ vector) is often a
215 subjective decision of the analyst. A higher order trend will fit the data better and hence
216 reduce the residuals and their variance. On the other hand, an ever-increasing trend flexibility
217 may lead to overfitting of the data, which means random noise and errors are included in the
218 statistical model, sacrificing its predictive power. Previous researchers have proposed the
219 Akaike's information criterion (AIC) (Akaike 1974) and the Bayesian information criterion
220 (BIC) (Schwarz 1978) as a means for model selection, both of which compare the changes
221 in log-likelihood value with respect to the number of associated model parameters. More
222 recently, Beck (2010) proposed the Bayesian system identification approach which evaluates
223 the expected information gain for individual model class. In the current study, the proposed
224 framework incorporates objective criteria to determine the optimal polynomial order for the
225 trend structure, balancing the needs for regression diagnostics, the significance of the high
226 order coefficients and the predictive power of the model.

227 *Significance of trend coefficients*

228 The current work adopts statistical hypothesis testing to assess the significance of trend
229 coefficients, in order to avoid overfitting of data. The basic idea is to test whether the highest
230 order trend coefficients are statistically different from zero, by calculating the Wald statistics
231 which are tested against the F -distribution. Two competing hypotheses are defined as: null
232 hypothesis H_0 – all highest order regression coefficients are zero; and alternative hypothesis
233 H_1 – at least one regression coefficient is nonzero, so that H_1 is the complement of H_0 . A
234 P_F value can be computed by comparing the Wald statistics to a $F(m, n-p)$ distribution,
235 where m is the number of the highest order coefficients. The highest order coefficients are

236 statistically significant with the acceptance of H_1 , indicated by a P_F value smaller than 0.05.
 237 Before executing statistical hypothesis testing, it is important to ensure the data follow a
 238 normal distribution, hence the necessity of the above-mentioned regression diagnostics.

239 *Leave-one-out cross validation*

240 The predictive power of a model can be evaluated through assessing the accuracy of its
 241 estimates by the “leave-one-out cross validation” method, which is performed by removing one
 242 observation at one time from the dataset, and then predicting its value using the remaining
 243 data (Haslett and Hayes 1998; Haslett 1999). During this process, the trend coefficients
 244 (β) and variance parameters ($\sigma_e^2 + \sigma_n^2$) may change with removal of each data point. The
 245 spatial correlation model, however, is assumed to remain constant, so there is no attempt to
 246 re-evaluate the correlation structure using REML. In this study, the cross validation scores,
 247 S_{cv} , is formulated based on the stacked vector for prediction errors, $\tilde{\epsilon}$, as below:

$$S_{cv} = \frac{(\tilde{\epsilon})^T \tilde{\epsilon}}{n} \quad (14)$$

248 S_{cv} defined herein can be interpreted as the average of squared prediction error at each
 249 borehole location under leave-one-out-cross validation. The advantage of this approach is
 250 that it does not require data partitioning, and hence minimizes perturbation to the data.
 251 It therefore provides an asymptotically unbiased estimate of the prediction errors, and is
 252 attractive for the purposes of model selection (Cawley and Talbot 2003).

253 **IMPLEMENTATION OF THE INTEGRATED FRAMEWORK**

254 Incorporating the components discussed in previous sections, the proposed framework
 255 ensures that the assumptions of REML are satisfied in geostatistical analyses of the data.
 256 Meanwhile, it allows objective determination of the order of trend polynomial and identification
 257 of potential outliers in the dataset. The predictive power of the model is also assessed through
 258 the leave-one-out cross validation method. While Fig. 2 shows the flowchart outlining the
 259 framework, its implementation can be summarised as follows:

- 260 1. The analysis starts with a linear trend structure (order $i = 1$). The autocovariance structure
261 (\mathbf{V}) and trend coefficients ($\hat{\beta}$) are estimated by REML (with Box-Cox transformation)
262 and GLS. Normality and constant variance checks are performed on the residuals.
- 263 2. A polynomial order i is rejected if either the normality or constant variance conditions is
264 violated. The analysis is then repeated with a $(i + 1)^{th}$ order polynomial for the trend
265 structure ($i = i + 1$).
- 266 3. If both normality and constant variance conditions are satisfied for the residuals, i becomes
267 a potential candidate. The significance of trend coefficients, $P_F(i)$, and cross validation
268 scores, $S_{cv}(i)$, will be evaluated for polynomial order i .
- 269 4. Meanwhile, the same analyses will be performed also on $(i + 1)^{th}$ order polynomial to
270 obtain $P_F(i + 1)$ and $S_{cv}(i + 1)$. If $P_F(i + 1)$ indicates non-significant polynomial order or
271 $S_{cv}(i) < S_{cv}(i + 1)$, then i is the optimal order for the trend structure.
- 272 5. If $P_F(i + 1)$ indicates a significant polynomial order, with $S_{cv}(i) > S_{cv}(i + 1)$ and normality
273 and constant variance conditions are satisfied, then order $i + 1$ replaces i as the potential
274 candidate ($i = i + 1$), and Step (4) onwards will be repeated.
- 275 6. Once the optimal polynomial order is determined for the trend structure, the \mathbf{V} and $\hat{\beta}$
276 estimates become final. Outliers in the dataset are also determined.

277 CASE STUDIES

278 Study regions and site descriptions

279 The proposed integrated framework is applied to analyze the spatial variability of engi-
280 neering rockhead levels at two project sites in Hong Kong, namely the Ngau Tau Kok (NTK)
281 site and the Cheung Wang Estate (CWE) site. Borehole information at the two sites was
282 obtained from geotechnical investigation reports of previous government projects in the areas,
283 which were archived in the Civil Engineering Library maintained by the Civil Engineering and
284 Development Department of the Hong Kong Government. For both cases, the boreholes are
285 irregularly spaced across the site, and the focus of the analysis is on the level of moderately

286 decomposed granite, referred to as Grade III material (GEO 1988) and commonly taken as
287 the rockhead level in the local practice.

288 Table 1 summarizes the sampling information for the two cases, including the areas of
289 the project sites and the sample sizes (i.e., number of boreholes). In addition, previous
290 geotechnical investigation had revealed the existence of a geological fault across the site of
291 CWE. To understand the effects of faults on spatial variability features, two sub-regional
292 blocks were extracted from CWE, with the fault crossing Block 1 but not Block 2. Details of
293 the analyses will be presented in the following sections where the benefits of the proposed
294 framework are also illustrated. It should be noted that the proposed approach will not replace
295 conventional geotechnical investigation techniques in identifying rockhead level or existence of
296 fault zones. However, it provides ‘added value’ to existing borehole information by revealing
297 the spatial characteristics and uncertainties regarding these geological features.

298 **NTK study site**

299 The NTK site is located in the eastern part of Hong Kong, where data from 150 boreholes
300 have been collected over an area of 650 m × 450 m. Spatial variations on the level of
301 engineering bedrock, i.e., Grade III moderately weathered granite at the site, are analyzed
302 using the proposed framework outlined in previous sections. To illustrate the importance of
303 residual diagnostics, and to elucidate the effects of assumptions on trend structures, Table 2
304 compares the analyses with different polynomial orders for the trend, with and without the
305 Box-Cox transformation. It should be noted that the proposed framework already incorporates
306 the selection criteria without the need to individually examine and compare each separate
307 analysis. The main purpose of Table 2 is to shed insights through the comparisons and allow
308 meaningful discussions on the significance of the proposed framework.

309 For illustration purposes, two series of analyses were performed, the first with Box-Cox
310 transformation of the raw data of rockhead level, and the second without. For each series,
311 the order of trend structure was varied from $i = 1$ (linear trend) to $i = 4$ (quartic trend) in
312 the REML analyses. Normality and constant variance tests were then conducted based on

313 the recovered residuals and Pearson residuals, respectively, with P_N and P_C values exceeding
314 0.05 indicating satisfaction of these conditions, as described earlier.

315 Table 2 shows that normality condition is in fact satisfied in all cases. However, without
316 Box-Cox transformation of the data, the condition of constant variance is not satisfied with
317 any trend structure. In other words, the REML (or other geostatistical) analyses are not
318 representative in those cases as the variance ($\sigma_e^2 + \sigma_n^2$) changes across various locations of the
319 domain. This issue will be discussed again in later sections on trend structure selection.

320 According to the proposed framework, the cubic trend structure ($i = 3$) was adopted
321 since its residuals satisfied the normality and constant variance tests, and it produced better
322 prediction than the 4th order polynomial based on the leave-one-out cross validation scores.
323 With this optimal trend structure, the autocovariance structure for rockhead variations is
324 estimated by REML and shown in Fig. 3(b). The estimates by method of moments are
325 also provided for comparison purposes, and the two methods produce similar results of
326 autocovariance structures.

327 Using Eqs. (8) and (9), predictions can be made at unsampled locations and the cor-
328 responding prediction variances (uncertainties) can be quantified, as shown in Fig. 3(c).
329 The prediction variance (σ_z^2) may be interpreted as the confidence level in the estimated
330 rockhead levels at unsampled locations, which varies spatially across the site according to the
331 autocorrelation structure and locations of existing boreholes. It contains contributions from
332 both uncertainties in deterministic trend structure and the corresponding residual effects. In
333 general, the prediction variance is low near sampled locations and increases with distance
334 away from boreholes. Such contour can provide guidance to determine the locations of
335 additional sampling points (if necessary), in order to achieve a specific level of confidence in
336 the predictions.

337 To illustrate the validity of σ_z^2 estimates, the leave-one-out cross validation method is again
338 applied, where the prediction error ($\tilde{\varepsilon}$) at location x is normalized by $\sigma_z(x)$, estimated with
339 $z(x)$ removed from the dataset. Fig. 3(d) shows the histogram of such normalized prediction

340 errors for all observation points, which broadly follows the standard normal distribution
341 curve. This implies that σ_z^2 provides reasonable estimates on the prediction uncertainties at
342 unsampled locations. While Figs. 3(c) and (d) show the results in the transformed space,
343 similar patterns are observed for the back-transformed prediction variance by Eq. (10), and
344 the associated normalized prediction errors, as presented in Figs. 3(e) and (f).

345 Influence of trend structure determination

346 Table 2 shows that the autocorrelation structure is highly influenced by the polynomial
347 order of the trend structure. In the current study, the optimal trend is selected with
348 considerations on the residual diagnostics, significance of trend coefficients (P_F), and leave-
349 one-out cross validation scores (S_{cv}), which shows whether over-fitting of the data has
350 occurred.

351 In general, a high order trend tends to match the existing observation points (\mathbf{z}) more
352 closely, therefore reducing the magnitudes of residuals (ε) and their variances. Closer
353 examination on Table 2 also reveals that higher polynomial orders are associated with smaller
354 scales of fluctuation (δ) and spatial dependence values (s). This is because with an increasing
355 polynomial order i , the trend structure becomes more flexible and the effective range of
356 residuals becomes shorter. Also, with increasing i , the smooth scale variation (σ_e^2) is reduced
357 due to better ‘fitting’ of the existing data. Meanwhile, the white noise effects (σ_n^2) are
358 also reduced since high order polynomials tend to ‘absorb’ some of the random noise in
359 measurements. As σ_e^2 decreases at a greater rate than σ_n^2 , the s value also reduces with
360 increasing i .

361 To further illustrate the importance of residual diagnostics in trend order determination,
362 Fig. 4 compares the diagnostics of recovered residuals under linear and cubic trends. The
363 histograms of recovered residuals show that normality conditions are satisfied for both trend
364 orders. With a sufficient sample size, the complexity of trend structure does not seem to
365 affect the normality of residuals.

366 On the contrary, constant variance tests based on the two trend structures produce

367 different results, with the cubic trend—but not the linear trend—satisfying constant variance
368 conditions. Plots of Pearson residuals along the north-south (N-S) and east-west (E-W)
369 directions are shown in Fig. 4. With a linear trend structure, the magnitudes of residuals
370 gradually diverge along both the N-S and E-W directions, implying that a potential trend
371 is still hidden in the residuals which masks the correlation features of the data, even after
372 filtering the linear trend component. On the other hand, the Pearson residuals under cubic
373 trend structure uniformly distribute around the zero axis along the two directions, indicating
374 that no significant trend exists among the residuals. The REML analyses are therefore
375 representative since $\sigma_e^2 + \sigma_n^2$ can be considered as constant throughout the study domain or
376 project site.

377 **Potential outliers at NTK site**

378 In the current study, outliers are defined as the data points with large deviations from
379 the trend (based on their residuals), and those that significantly influence the trend structure
380 (based on their Cook's distances). By implementing the proposed integrated framework, eight
381 outliers are identified with the optimal (cubic) trend structure.

382 Figs. 5(a) and (b) show the locations of outliers identified by the two approaches. Four
383 outliers (No. 1 – 4) are identified based on the Cook's distances, and Fig. 5(c) shows the
384 magnitudes of the residuals for two of them, compared to their neighboring points. When
385 examining the residuals, significant differences can be observed between the outliers and
386 their neighbors, which explain their substantial influence on the regression coefficients and
387 hence large values of Cook's distances. However, such influence may not be obvious by
388 only examining their corresponding raw data values. This shows that although outliers are
389 associated with significantly different residuals, they may not be easily detected when the
390 sample size is large, such as in the NTK site with 150 borehole records.

391 A potential deficiency of this approach is that the Cook's distances can be affected by the
392 leverage effect: a data point near the edge of the sampling domain tends to demonstrate a
393 higher influence on the regression coefficients than those near the central region. To supplement

394 the Cook's distance method, the residual values are also examined in the current study,
395 and those exceeding ± 1.96 times their standard deviation are also considered as potential
396 outliers (Fig. 5(d)), as they represent 'extreme' values outside the 95% inter-percentile range
397 (assuming normal distribution). It should be noted that among those data points, two clusters
398 are identified at NTK, where groups of boreholes spatially close to each other have similar
399 values of residuals. They may be manifestations of local rockhead variations that are not
400 captured by the large-scale trend, instead of results of measurement errors. The proposed
401 framework thereby allows such details to be revealed so that engineers and geologists can
402 focus on a small number of potential outliers to ensure accuracy and consistency of the
403 dataset.

404 In addition, Table 2 shows that the number of potential outliers are affected by the
405 adopted trend structure. In general, with a higher order polynomial, the trend involves
406 greater flexibility and hence a larger number of 'influential' data points may be identified
407 as outliers. In many cases, the data points identified as outliers using the low order trend
408 are also outliers under higher order trend structure. The current approach is established to
409 automatically identify these statistical influential or extreme points, so they can be reviewed
410 again by engineers or geologists to determine whether they indeed contain measurement
411 errors or mistakes.

412 **CWE study site and effects of faults**

413 The second study site is located at the Cheung Wang Estate (CWE) on the Tsing Yi
414 Island in Hong Kong. A total number of 321 borehole records were obtained within an
415 area of $800 \text{ m} \times 500 \text{ m}$, and the variations of Grade III moderately weathered granite was
416 studied. At the CWE site, a geological fault has been reported from previous geotechnical
417 investigation. Effects of the fault on the spatial variability of rockhead level are also evaluated
418 in the current study.

419 Geological faults often form discontinuities in the rockhead level, which may have significant
420 implications on the design and construction of an engineering project. As shown in Fig. 6(a)

421 and (c), one NW-SE fault cuts through the western part of the CWE site. To understand
422 the influence of the fault, two sub-regional blocks were extracted from the CWE site, with
423 the same sample domain size and similar sampling densities. The borehole locations and
424 partition scheme of the blocks are also illustrated in Fig. 6(a). Block 1 is designed to be
425 intersected by the fault, while Block 2 is deemed to be free of its influence.

426 Table 3 compares the spatial variation features of the two blocks. At the CWE study site,
427 the fault is associated with reductions in scale of fluctuation (δ) (about 50%) and in spatial
428 dependence (s) (about 20%) , which imply higher levels of uncertainties in the rockhead
429 levels. The differences in the two autocorrelation structures and prediction variances are
430 also shown in Figs. 6(b) and (d), respectively. Intuitively, the existence of geological faults
431 or other discontinuities at the site will increase the uncertainty in the subsurface profiles.
432 Analyses by the proposed framework provide a quantitative evaluation of such effects, which
433 may then be coupled with risk analyses by reliability methods.

434 DISCUSSIONS

435 The framework proposed in the current study ensures that spatial correlation analyses
436 performed on geotechnical data satisfy the fundamental assumptions of REML and are
437 statistical sound. A key feature of the framework is the methodological and objective
438 determination of the optimal trend structure. As shown in Table 2 and discussed by Lark
439 and Webster (2006), residual analyses can be substantially affected by the choice of trend
440 structure. The proposed framework involves holistic considerations on the significance of
441 trend coefficients and variance distributions of the residuals, which lead to rational decisions
442 on the trend component in the analyses.

443 The proposed framework also offers simple and automatic detection of potential outliers
444 or errors in the dataset, through the Cook's distances of the data points and distribution
445 of their residuals. Automatic detection of outliers is especially beneficial in the case of a
446 large dataset, where anomalies may not be easily identified manually. The potential outliers
447 identified using the current approach can be reviewed again by engineers or geologists, who

448 can then determine whether they indeed involve measurement errors or human mistakes.

449 Using the BLUP technique (Eqs. (8)) and (9)), contours of the prediction variances can
450 be produced to quantify the level of confidence in predictions at unsampled locations. This
451 can form a useful guidance to determine necessity and/or locations of additional sampling.
452 In addition, the predicted properties and prediction variance from BLUP can be used to
453 construct a conditional random field (Li et al. 2016; Lo and Leung 2016), to be adopted
454 for probabilistic geotechnical models by Random Finite Element Method (RFEM)(Fenton
455 and Griffiths 2003; Griffiths et al. 2009). By quantifying the spatial uncertainty around the
456 observed data points, predictions of the probabilistic models can be more precise than those
457 using an unconditional random field.

458 It should be noted that the presented case studies involve large numbers of boreholes
459 (150 to 350), and the current study aims to fully utilize such information to demonstrate
460 the proposed framework and reveal spatial correlation features of the rockhead profile. This,
461 however, does not imply that the approach is only applicable to such sample sizes. While
462 any statistical analysis will improve with a large sample size, the proposed method will
463 also produce more robust results in smaller dataset than traditional method of moments or
464 maximum likelihood methods, due to the rigorous consideration of stationarity requirements,
465 detrending and detection of outliers.

466 To illustrate the robustness of the proposed framework, Block 1 of the CWE case is taken
467 as an example where 100 subsets are extracted, each containing 50% of data points randomly
468 chosen from the original dataset. These 100 subsets are analysed using both the proposed
469 framework and the approach in Liu and Leung (2015), which consists of REML but not the
470 other key features of this study such as data transformation, regression diagnostics, trend
471 order determination and outlier detection. Fig. 7 compares the statistics of the two series
472 of analyses, and shows that the proposed framework produces closer estimates of spatial
473 dependence and scale of fluctuation compared to results from the complete dataset, and are
474 associated with smaller variances which indicate more robust analyses. In addition, the cross

475 validation scores are generally lower under the proposed framework. Fig. 7(d) also shows
476 an analysis on one subset using the method of moments with different lag sizes. Traditional
477 method of moments does not include simultaneous determination of the large scale trend, so
478 in this case the trend is adopted from REML analysis. Even so, estimates by the method of
479 moments are shown to be dependent on subjective decisions on lag size and curve-fitting for
480 the spatial correlation parameters.

481 **CONCLUSION**

482 This paper presents an integrated framework for geostatistical analyses, incorporating the
483 REML method with the Matérn autocovariance model, to estimate the spatial correlation
484 features of rockhead levels. The approach is a robust technique which includes efficient
485 determination of optimal trend structure and identification of spatial outliers, meanwhile
486 ensuring the basic premises of REML, including assumptions on normality and constant
487 variance of residuals, are satisfied across the study region.

488 The framework is demonstrated through analyses on the spatial variations of Grade III
489 rockhead levels using borehole data from two sites in Hong Kong. As illustrated in the CWE
490 case, geological faults can have significant influences on the spatial variability features of
491 rockhead levels. In particular, the scale of fluctuation and spatial dependence reduce with
492 existence of faults, which corresponds to higher spatial uncertainty. It is recommended that
493 sub-regional analyses be performed separately whenever local geological features are identified
494 at the project site.

495 **ACKNOWLEDGEMENTS**

496 The work presented in this paper is financially supported by the Research Grants Council
497 of the Hong Kong Special Administrative Region (Project No. 25201214). Also, the authors
498 would like to acknowledge the permission of the Civil Engineering and Development Depart-
499 ment, the Government of Hong Kong Special Administrative Region, to present analyses of
500 data obtained from the Civil Engineering Library. Readers may contact the corresponding
501 author for details of the dataset used in the study.

REFERENCES

- Akaike, H. 1974. "A new look at the statistical model identification." *IEEE Transactions on Automatic Control*, 19(6), 716–723.
- Atkinson, P. M., Pardo-Iguzquiza, E., and Chica-Olmo, M. 2008. "Downscaling cokriging for super-resolution mapping of continua in remotely sensed images." *Geoscience and Remote Sensing, IEEE Transactions on*, 46(2), 573–580.
- Beck, J. L. 2010. "Bayesian system identification based on probability logic." *Structural Control and Health Monitoring*, 17(7), 825–847.
- Belsley, D. A., Kuh, E., and Welsch, R. E. 2005. *Regression diagnostics: Identifying influential data and sources of collinearity*, Vol. 571. John Wiley & Sons.
- Box, G. E. P. and Cox, D. R. 1964. "An analysis of transformations." *Journal of the Royal Statistical Society, Series B (Methodological)*, 26(2), 211–252.
- Breusch, T. S. and Pagan, A. R. 1979. "A simple test for heteroscedasticity and random coefficient variation." *Econometrica: Journal of the Econometric Society*, 1287–1294.
- Cao, Z. and Wang, Y. 2013. "Bayesian approach for probabilistic site characterization using cone penetration tests." *Journal of Geotechnical and Geoenvironmental Engineering*, 139(2), 267–276.
- Cao, Z. and Wang, Y. 2014. "Bayesian model comparison and selection of spatial correlation functions for soil parameters." *Structural Safety*, 49, 10 – 17 Special Issue In Honor of Professor Wilson H. Tang.
- Cawley, G. C. and Talbot, N. L. 2003. "Efficient leave-one-out cross-validation of kernel fisher discriminant classifiers." *Pattern Recognition*, 36(11), 2585–2592.
- Chiasson, P., Lafleur, J., Soulié, M., and Law, K. T. 1995. "Characterizing spatial variability of a clay by geostatistics." *Canadian Geotechnical Journal*, 32(1), 1–10.
- Christian, J. T. and Baecher, G. B. 2011. "Unresolved problems in geotechnical risk and reliability." *ASCE GSP 224: Geo-Risk 2011: Risk Assessment and Management*, 50–63.

- Clayton, C. R. I. 2001. *Managing geotechnical risk: improving productivity in UK building and construction*. Thomas Telford.
- Cook, R. D. 1977. "Detection of influential observation in linear regression." *Technometrics*, 19(1), 15–18.
- Cressie, N. and Lahiri, S. N. 1996. "Asymptotics for reml estimation of spatial covariance parameters." *Journal of Statistical Planning and Inference*, 50(3), 327–341.
- Cressie, N. A. C. 1993. *Statistics for Spatial Data (Revised Edition)*. John Wiley & Sons.
- Dasaka, S. M. and Zhang, L. M. 2012. "Spatial variability of in situ weathered soil." *Géotechnique*, 62(5), 375–384.
- DeGroot, D. J. 1996. "Analyzing spatial variability of in situ soil properties." *Uncertainty in the Geologic Environment: From Theory to Practice*, Vol. 1, 210–238.
- DeGroot, D. J. and Baecher, G. B. 1993. "Estimating autocovariance of in-situ soil properties." *Journal of Geotechnical Engineering*, 119(1), 147–166.
- Elkateb, T., Chalaturnyk, R., and Robertson, P. K. 2003. "An overview of soil heterogeneity: quantification and implications on geotechnical field problems." *Canadian Geotechnical Journal*, 40(1), 1–15.
- Fenton, G. A. and Griffiths, D. V. 2003. "Bearing-capacity prediction of spatially random c - ϕ soils." *Canadian Geotechnical Journal*, 40(1), 54–65.
- Firouzianbandpey, S., Griffiths, D. V., Ibsen, L. B., and Andersen, L. V. 2014. "Spatial correlation length of normalized cone data in sand: case study in the north of denmark." *Canadian Geotechnical Journal*, 51(8), 844–857.
- GEO 1988. *GEOGUIDE 3: Guide to Rock and Soil Descriptions*. Geotechnical Engineering Office, Civil Engineering Department, Government of Hong Kong.
- Griffiths, D., Huang, J., and Fenton, G. 2009. "Influence of spatial variability on slope reliability using 2-d random fields." *Journal of Geotechnical and Geoenvironmental Engineering*, 135(10), 1367–1378.

- Haskard, K. A. 2007. *An anisotropic Matérn spatial covariance model: REML estimation and properties*. Ph.D. thesis, The University of Adelaide.
- Haslett, J. 1999. "A simple derivation of deletion diagnostic results for the general linear model with correlated errors." *Journal of the Royal Statistical Society: Series B (Statistical Methodology)*, 61(3), 603–609.
- Haslett, J. and Hayes, K. 1998. "Residuals for the linear model with general covariance structure." *Journal of the Royal Statistical Society. Series B, Statistical Methodology*, 201–215.
- Jensen, D. R. and Ramirez, D. E. 1999. "Recovered errors and normal diagnostics in regression." *Metrika*, 49(2), 107–119.
- Lark, R. 2000. "Estimating variograms of soil properties by the method-of-moments and maximum likelihood." *European Journal of Soil Science*, 51(4), 717–728.
- Lark, R., Cullis, B., and Welham, S. 2006. "On spatial prediction of soil properties in the presence of a spatial trend: the empirical best linear unbiased predictor (e-blup) with reml." *European Journal of Soil Science*, 57(6), 787–799.
- Lark, R. M. and Cullis, B. R. 2004. "Model-based analysis using reml for inference from systematically sampled data on soil." *European Journal of Soil Science*, 55(4), 799–813.
- Lark, R. M. and Webster, R. 2006. "Geostatistical mapping of geomorphic variables in the presence of trend." *Earth Surface Processes and Landforms*, 31(7), 862–874.
- Li, X., Zhang, L., and Li, J. 2016. "Using conditioned random field to characterize the variability of geologic profiles." *Journal of Geotechnical and Geoenvironmental Engineering*, 142(4), 04015096.
- Liu, W. F. and Leung, Y. F. 2015. "Analyzing spatial variability of geologic profiles for four sites in Hong Kong." *The 5th International Symposium on Geotechnical Safety and Risk, Rotterdam, The Netherlands*, 157–162.
- Lo, M. K. and Leung, Y. F. 2016. "Bayesian updating of subsurface spatial correlation

- through monitoring of infrastructure and building developments.” *International Conference on Smart Infrastructure and Construction, Cambridge, United Kingdom*, (Accepted).
- Matérn, B. 1960. “Stochastic models and their application to some problems in forest surveys and other sampling investigations.” *Meddelanden från Statens Skogsforskningsinstitut*, 49(5), 1–144.
- Matheron, G. 1971. *The theory of regionalized variables and its application*. Fontainebleau, France.
- Minasny, B. and McBratney, A. B. 2005. “The Matérn function as a general model for soil variograms.” *Geoderma*, 128(3-4), 192–207.
- Nieuwenhuis, R., te Grotenhuis, H., and Pelzer, B. 2012. “Influence. me: tools for detecting influential data in mixed effects models.” *The R Journal*, 38–47.
- Phoon, K. K. and Kulhawy, F. H. 1999a. “Characterization of geotechnical variability.” *Canadian Geotechnical Journal*, 36(4), 612–624.
- Phoon, K. K. and Kulhawy, F. H. 1999b. “Evaluation of geotechnical property variability.” *Canadian Geotechnical Journal*, 36(4), 625–639.
- Phoon, K.-K., Quek, S.-T., and An, P. 2003. “Identification of statistically homogeneous soil layers using modified bartlett statistics.” *Journal of Geotechnical and Geoenvironmental Engineering*, 129(7), 649–659.
- Phoon, K.-K., Quek, S.-T., and An, P. 2004. “Geostatistical analysis of cone penetration test (cpt) sounding using the modified bartlett test.” *Canadian Geotechnical Journal*, 41(2), 356–365.
- Rue, H. and Held, L. 2005. *Gaussian Markov Random Fields: Theory and Applications*. CRC Press, Taylor and Francis.
- Santra, P., Das, B. S., and Chakravarty, D. 2012. “Spatial prediction of soil properties in a watershed scale through maximum likelihood approach.” *Environmental Earth Sciences*, 65(7), 2051–2061.
- Schwarz, G. 1978. “Estimating the dimension of a model.” *Ann. Statist.*, 6(2), 461–464.

- Smirnov, N. 1939. "On the estimation of the discrepancy between empirical curves of distribution for two independent samples." *Bulletin Mathématique de l'Université de Moscou*, 2, 3–14.
- Soulié, M., Montes, P., and Silvestri, V. 1990. "Modeling spatial variability of soil parameters." *Canadian Geotechnical Journal*, 27(5), 617–630.
- Stein, M. L. 1999. *Interpolation of Spatial Data: Some Theory for Kriging*. Springer.
- Storn, R. and Price, K. 1997. "Differential evolution — a simple and efficient heuristic for global optimization over continuous spaces." *Journal of Global Optimization*, 11(4), 341–359.
- Stuedlein, A. W., Kramer, S. L., Arduino, P., and Holtz, R. D. 2012. "Geotechnical characterization and random field modeling of desiccated clay." *Journal of Geotechnical and Geoenvironmental Engineering*, 138(11), 1301–1313.
- Vanmarcke, E. H. 1977. "Probabilistic modeling of soil profiles." *ASCE Journal of Geotechnical Engineering Division*, 103(GT11), 1227–1246.
- Wang, Y., Au, S.-K., and Cao, Z. 2010. "Bayesian approach for probabilistic characterization of sand friction angles." *Engineering Geology*, 114(34), 354 – 363.
- Wang, Y., Cao, Z., and Li, D. 2016. "Bayesian perspective on geotechnical variability and site characterization." *Engineering Geology*, 203, 117 – 125 Special Issue on Probabilistic and Soft Computing Methods for Engineering Geology.
- Wang, Y., Huang, K., and Cao, Z. 2013. "Probabilistic identification of underground soil stratification using cone penetration tests." *Canadian Geotechnical Journal*, 50(7), 766–776.
- Wang, Y., Huang, K., and Cao, Z. 2014. "Bayesian identification of soil strata in london clay." *Géotechnique*, 64(3), 239–246.
- Wang, Y., Zhao, T., and Cao, Z. 2015. "Site-specific probability distribution of geotechnical properties." *Computers and Geotechnics*, 70, 159 – 168.
- Wang, Y.-J. and Chiasson, P. 2006. "Stochastic stability analysis of a test excavation involving spatially variable subsoil." *Canadian Geotechnical Journal*, 43(10), 1074–1087.

List of Tables

1 Domain scales and sample sizes for two cases 28

2 Comparisons of spatial correlation analyses for NTK site 29

3 Effects of geological faults on spatial correlation features 30

Draft

TABLE 1. Domain scales and sample sizes for two cases

Case study	Area of domain	Sample size
NTK	650 m × 450 m	150
CWE	Block 1 (with fault)	360 m × 400 m
	Block 2 (no fault)	360 m × 400 m

TABLE 2. Comparisons of spatial correlation analyses for NTK site

Case	Trend order (<i>i</i>)	Spatial dependence (<i>s</i>)	Scale of fluctuation (δ)	Constant variance test (P_C)	Normality test (P_N)	Trend coefficients test (P_F)	No. of potential outliers	Cross validation score (S_{cv})
NTK (transformed)	1	0.93	308 m	0.0010(N)	0.3041(Y)	0.0183(Y)	1	27.49
	2	0.89	227 m	0.0102(N)	0.7123(Y)	0.2226(N)	4	28.42
	3	0.75	125 m	0.2700(Y)	0.7250(Y)	2.71×10^{-6} (Y)	8	31.95
	4	0.58	70 m	0.5995(Y)	0.3459(Y)	3.30×10^{-10} (Y)	10	33.50
NTK (raw data)	1	0.94	273 m	0.0005(N)	0.5540(Y)	0.0088(Y)	5	28.48
	2	0.90	215 m	0.0008(N)	0.5908(Y)	0.2384 (N)	8	29.29
	3	0.74	128 m	0.00001(N)	0.3063(Y)	8.17×10^{-6} (Y)	10	32.99
	4	0.65	96 m	0.0004(N)	0.2752(Y)	2.11×10^{-6} (Y)	15	35.44

TABLE 3. Effects of geological faults on spatial correlation features

CWE sub-regional block	Optimal trend order	Scale of fluctuation (δ)	Spatial dependence (s)
Block 1 (with fault)	2 (quadratic)	74 m	0.53
Block 2 (no fault)	2 (quadratic)	143 m	0.64

List of Figures

1	Relationship between scale of fluctuation, δ , and Matérn function parameters, ν and r	32
2	Flowchart of integrated residual analysis framework	33
3	(a) Rockhead level; (b) Autocovariance structure; (c,d) Prediction variance contour and normalized prediction errors in transformed space; (e,f) Prediction variance contour and normalized prediction errors in back-transformed original space	34
4	Residual analyses for NTK site under linear and cubic trend assumptions . .	35
5	(a,b) Locations of potential outliers identified by (c) Cook's distances and (d) residual analysis	36
6	(a) Two sub-regional blocks at CWE site; (b) Autocorrelation structures for two blocks; (c) Variations in rockhead levels; (d) Prediction variance contours for two blocks	37
7	Analyses of subsets by the proposed framework, the REML approach adopted in Liu and Leung (2015) and method of moments	38

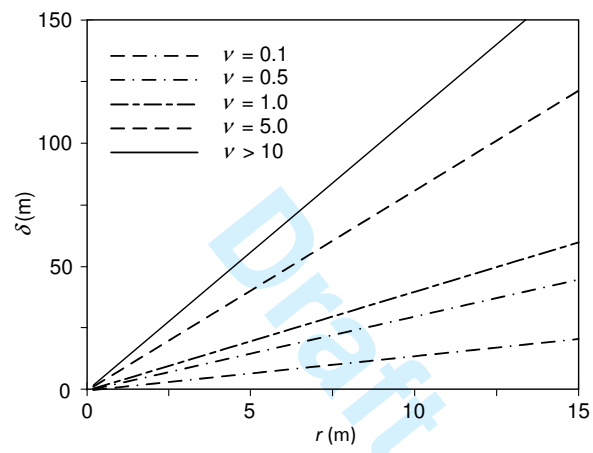


FIG. 1. Relationship between scale of fluctuation, δ , and Matérn function parameters, ν and r

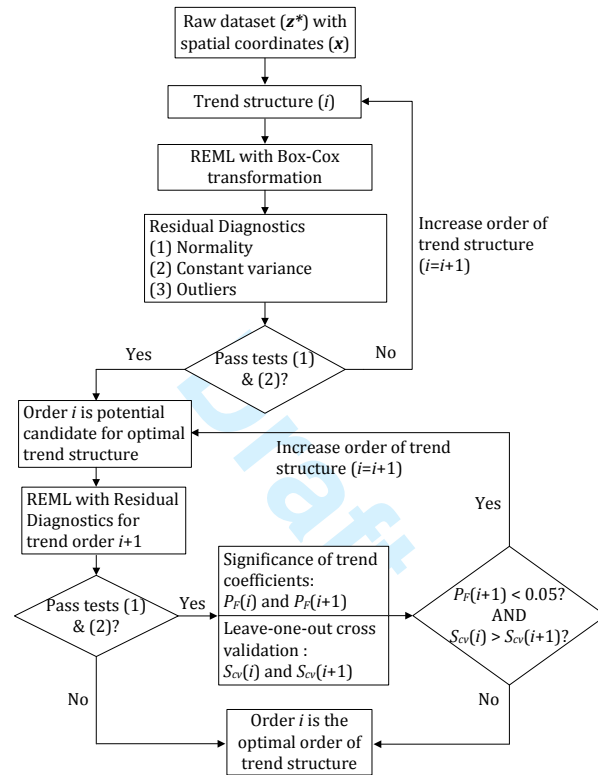


FIG. 2. Flowchart of integrated residual analysis framework

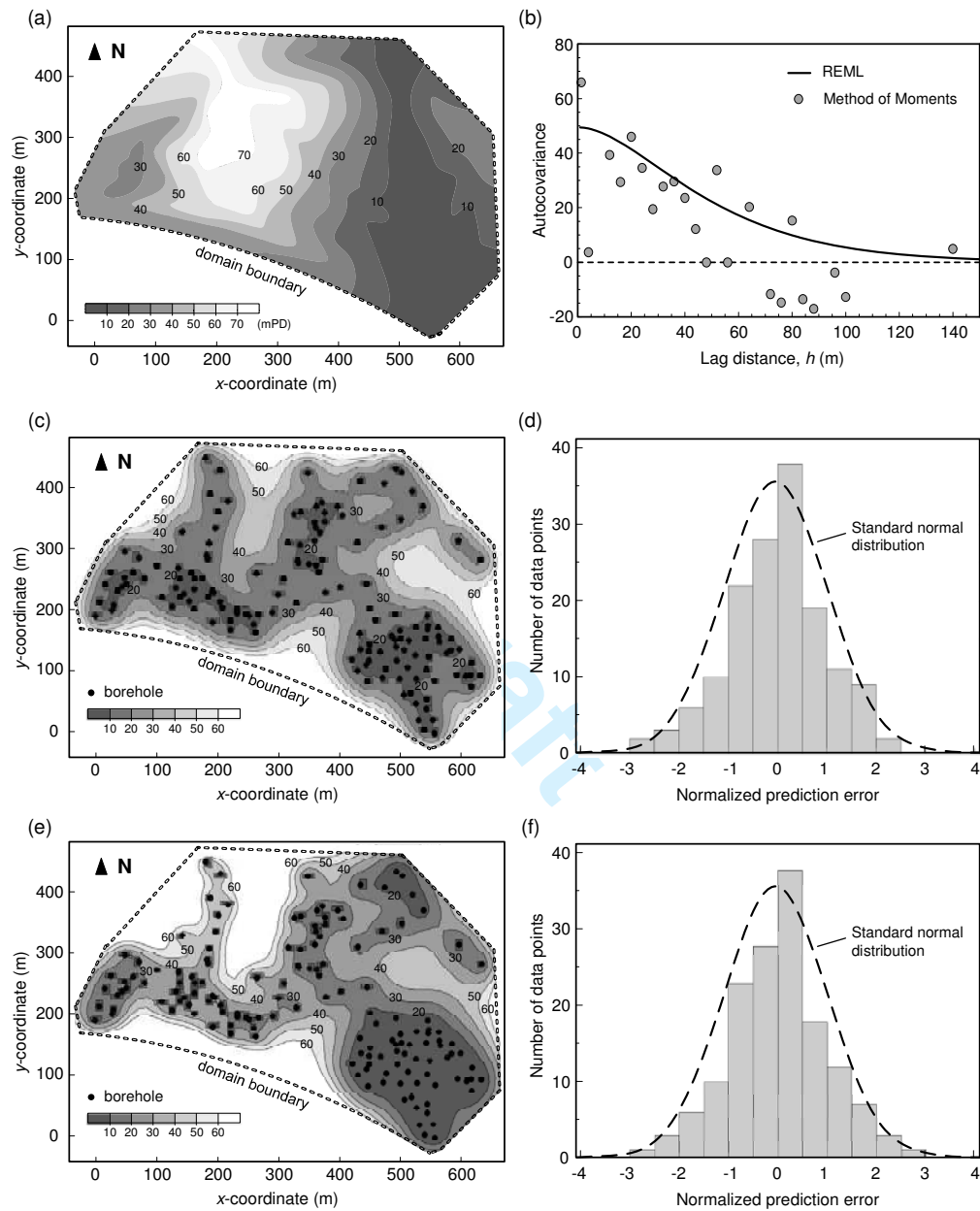


FIG. 3. (a) Rockhead level; (b) Autocovariance structure; (c,d) Prediction variance contour and normalized prediction errors in transformed space; (e,f) Prediction variance contour and normalized prediction errors in back-transformed original space

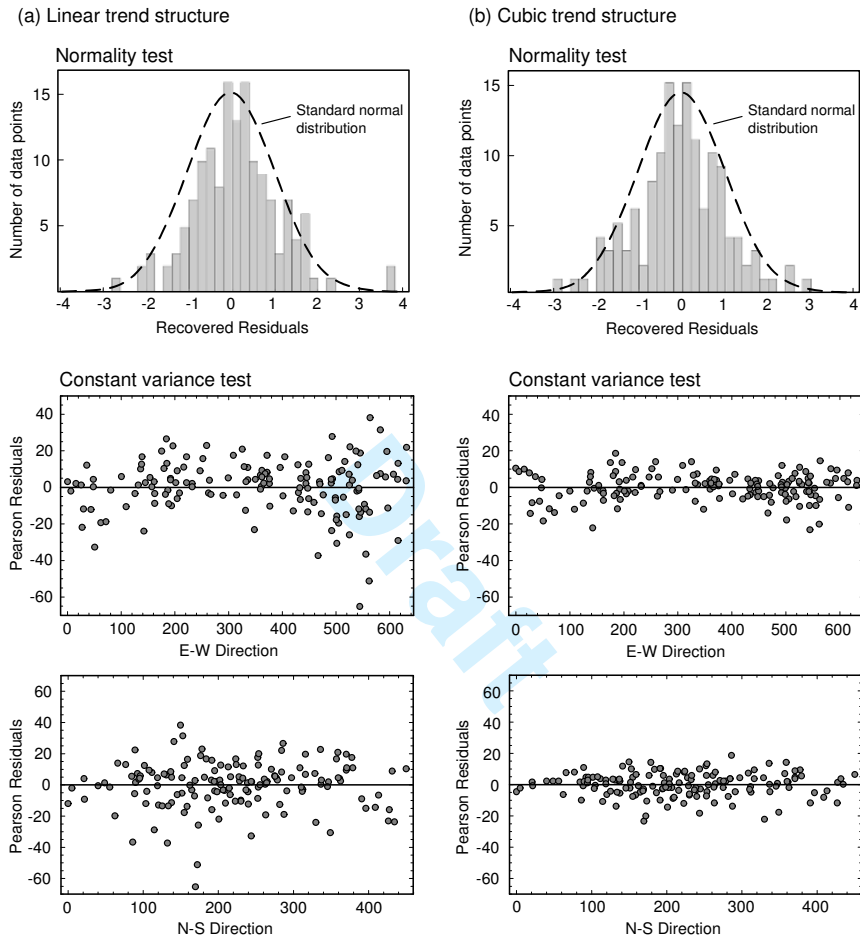


FIG. 4. Residual analyses for NTK site under linear and cubic trend assumptions

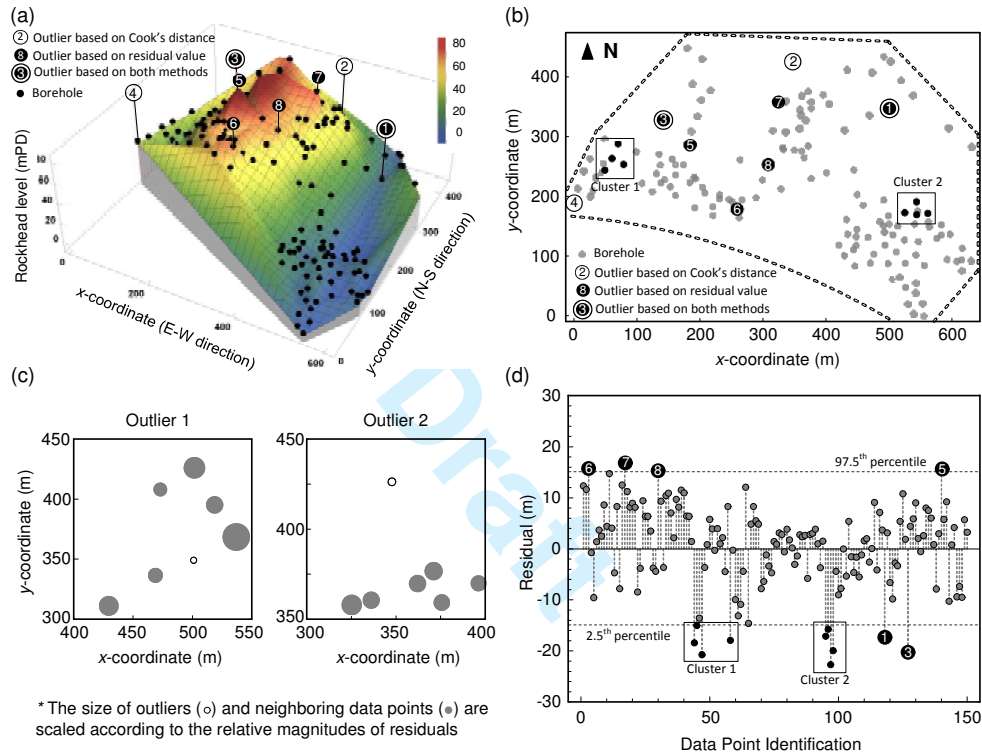


FIG. 5. (a,b) Locations of potential outliers identified by (c) Cook's distances and (d) residual analysis

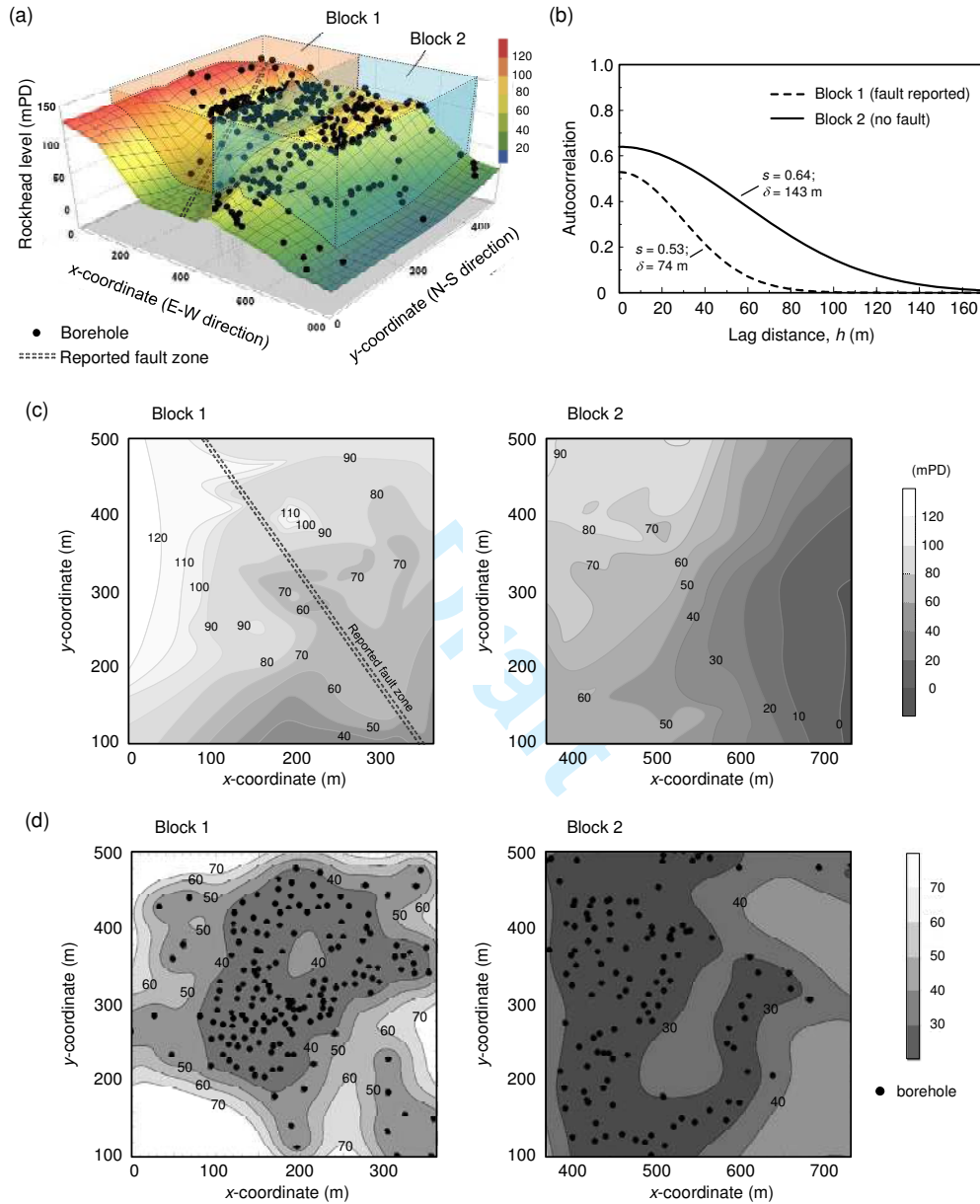


FIG. 6. (a) Two sub-regional blocks at CWE site; (b) Autocorrelation structures for two blocks; (c) Variations in rockhead levels; (d) Prediction variance contours for two blocks

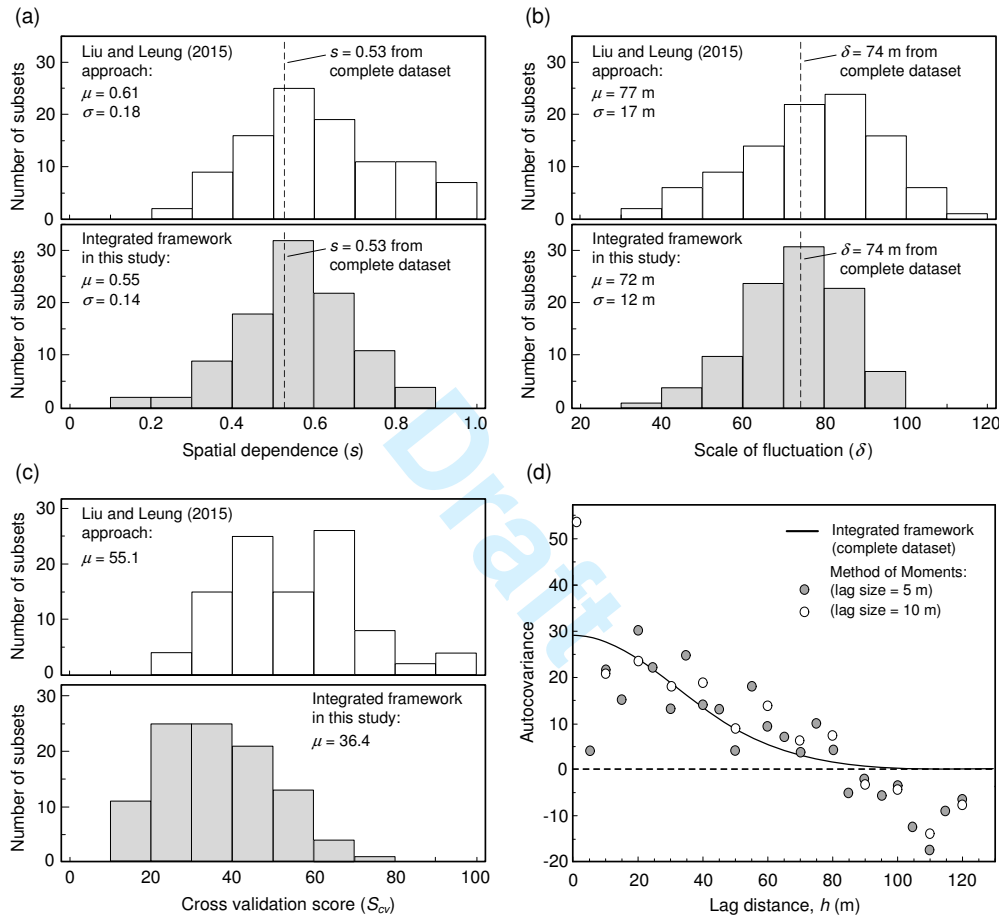


FIG. 7. Analyses of subsets by the proposed framework, the REML approach adopted in Liu and Leung (2015) and method of moments